SulA inhibits assembly of FtsZ by a simple sequestration mechanism

Yaodong Chen[1], **Sara L. Milam**, and **Harold P. Erickson**[2]
Department of Cell Biology, Duke University Medical Center, Durham, NC 27710-3709

Abstract

We have investigated the inhibition by SulA of the assembly of *Escherichia coli* FtsZ. Using quantitative GTPase and fluorescence assays, we found that SulA inhibition resulted in an increase in the apparent critical concentration for FtsZ assembly. The increase in apparent critical concentration was always less than the total amount of SulA added, suggesting that the association of SulA and FtsZ was of modest affinity. Isothermal titration calorimetry gave a value of 0.78 μM for the dissociation constant of the FtsZ-SulA complex, similar in magnitude to the 0.72 μM critical concentration of FtsZ protofilament assembly at steady state. We modeled the reaction as an equilibrium competition between (a) FtsZ subunits assembling onto protofilaments or (b) binding SulA. When FtsZ was assembled in GMPCPP or in EDTA, the inhibition of SulA was reduced. The reduced inhibition could be explained by a 3- and 10-fold weaker binding of SulA to FtsZ. The mutant D212G, which has no GTPase activity and therefore minimal subunit cycling, was shown here to assemble one-stranded protofilaments, and the assembly was blocked by SulA. We also assayed the SulA and FtsZ proteins from *Pseudomonas.* The SulA inhibition was stronger than with the *E.* coli proteins, and the model indicated a 5-fold higher affinity of *Pseudomonas* SulA for FtsZ.

FtsZ is a bacterial tubulin homolog and the major cytoskeletal protein involved in bacterial cell division. It assembles short, one-stranded protofilaments in vitro, and these are further assembled into a Z ring, which is tethered to the membrane at the site of cytokinesis. FtsZ provides not just the cytoskeletal framework, but also generates the constriction force, probably by a mechanism of protofilament bending (1–3). A dozen other proteins are involved in cytokinesis, most of them in remodeling the peptidoglycan layer. For a review of FtsZ see (4), and for a review of the accessory proteins and overall process see (5).

SulA is a small protein induced as part of the SOS response to DNA damage in *Escherichia coli* and related gram negative bacteria. SulA binds to FtsZ and blocks cell division until the DNA is repaired and SulA is proteolyzed (6–9). *E. coli* SulA protein is unstable in most in vitro conditions tested, but can be produced as a fusion with maltose binding protein (MBP) (10). In this original study MBP-SulA was toxic to *E. coli* in vivo (demonstrating activity) and bound to FtsZ in vitro, but appeared not to inhibit FtsZ GTPase activity (10). Two later studies provided convincing evidence that SulA fusion proteins inhibited FtsZ GTPase, but only about 50% at a 1:1 stoichiometry (11, 12).

In contrast to the instability of *E. coli* SulA, SulA from *Pseudomonas aeruginosa* can be expressed and purified as a soluble protein. A crystal structure of the complex of PaFtsZ and SulA (for clarity we will prefix the FtsZ with Ec or Pa where needed) showed the SulA bound to the bottom of FtsZ (13). The SulA made contact with the NxD of the synergy/T7

[2]Correspondence: h.erickson@cellbio.duke.edu, Tel: 919-684-6385, Fax: 919-684-8090.
[1]Current address: Department of Biology, University of North Carolina at Chapel Hill, Chapel Hill, NC 27599. ydchen@unc.edu

loop (NxDxxD), which is buried in the longitudinal interface in the protofilament. The bound SulA would therefore sterically block assembly. This structure thus suggests a simple model for SulA inhibition: it sequesters the FtsZ monomers to which it is bound, and reduces the effective concentration of active FtsZ.

A recent study of Dajkovic et al (14) used a sedimentation assay to measure EcFtsZ polymer over a range of FtsZ concentrations, and for various concentrations of MBP-SulA. They found that in the absence of SulA the critical concentration (Cc) for assembly was 0.9 μM, and the "apparent Cc" increased to 4.3 and 5.9 μM in the presence of 3.5 and 5.0 μM SulA. We will use the term "apparent Cc" (CcApp) to designate the elevated minimal concentration for assembly in the presence of SulA. As reported by Dajkovic et al (14), the reaction behaved as if the concentration of active FtsZ were equal to the total FtsZ minus the concentration of SulA. This is consistent with the sequestration mechanism, with one important assumption. The affinity for FtsZ for binding SulA must be much greater than the affinity of FtsZ for adding to a protofilament. The affinity of FtsZ for SulA has not been measured previously.

The sequestration mechanism was complicated by a remarkable discovery. Dajkovic et al (14) found that when FtsZ was assembled in GMPCPP instead of GTP, the assembly was no longer sensitive to SulA. GMPCPP is hydrolyzed very slowly, about 1/50 the rate of GTP (15). This suggested that GTP hydrolysis and associated cycling of subunits is required for inhibition by SulA. Consistent with this, the authors found that assembly was also insensitive to SulA when it was induced with GDP + AlF, which acts as a non-hydrolysable GTP analog, or in GTP plus EDTA, which chelates Mg and completely blocks GTP hydrolysis. This is not consistent with a simple sequestration mechanism. Dajkovic et al (14) concluded that inhibition by SulA only occurred when FtsZ was cycling subunits following GTP hydrolysis, and proposed a model based on two conformations of FtsZ. We have discussed potential problems with this model elsewhere (4).

The mutant D212G has almost no GTPase activity, and one would predict from the above conclusion that it would be insensitive to SulA inhibition. However D212 (the last D in the NxDxxD sequence) is outside the FtsZ-SulA interface (13), and a yeast two-hybrid study (14), as well as an affinity binding column assay (12) showed that it can bind SulA. Trusca et al (12) reported that assembly of D212G, when stabilized by DEAE dextran, was not inhibited by SulA. It has been thought that D212G cannot assemble protofilaments without DEAE dextran or an excess of wild type FtsZ (11), so this mutant was not tested in the Dajkovic et al study (14).

We have now re-examined this study using the sensitive and quantitative fluorescence assays we have recently developed (16–18). We also wanted to determine quantitatively the association constant for SulA binding FtsZ. The new data show that this binding is similar in affinity to that for FtsZ binding a protofilament. Our data can be explained by a new model, based on an equilibrium competition between free FtsZ subunits binding either protofilament ends or SulA.

EXPERIMENTAL PROCEDURES

Protein purification

Expression vectors for EcFtsZ and mutants were constructed using site-directed mutagenesis in the plasmid pET11b-FtsZ, and proteins were purified as described previously (16, 17). Briefly, the soluble bacterially expressed protein was purified by 30% ammonium sulfate precipitation, followed by chromatography on a source Q 10/10 column (GE healthcare)

with a linear gradient of 50–500 mM KCl in lysis buffer (50 mM Tris, pH 7.9, 1 mM EDTA, 10% glycerol). Peak fractions were identified by SDS-PAGE and stored at −80 °C.

The *E. coli* SulA expression vector, a pBAD vector that produces SulA fused at its N terminus to MBP was a gift from Joe Lutkenhaus (11). The vector was transformed into *E. coli* strain DH5α, and expression induced by 0.2% arabinose for 3 hr. The bacteria were suspended in lysis buffer, and the soluble MBP-SulA was bound to a column of Amylose resin (New England Biolabs, MA). The MBP-SulA was eluted with 10 mM maltose in lysis buffer, and applied to a source Q 10/10 column (GE healthcare) and eluted with a linear gradient of 50–500 mM KCl in lysis buffer. Peak fractions were identified by SDS-PAGE and stored at −80 °C.

The cDNA for PaFtsZ was obtained by PCR from genomic DNA and inserted into the plasmid pET-15b, which produces a His_6-tag at the N-terminus. Overexpressed His-PaFtsZ protein in 50 mM Tris, pH 7.4, 500 mM KCl was bound to a column of TALON Metal Affinity Resin (Clontech Laboratories, Inc.). The Histag protein was eluted with 10 mM EDTA. After incubation with thrombin to remove the His-tag, the protein was further purified by chromatography on a source Q 10/10 column (GE healthcare), similar to EcFtsZ. PaSulA was prepared by similar cloning and expression and was purified by the talon column. The Histag PaSulA protein was insoluble at high concentration and was usually stored below 30 μM.

FtsZ assembly assays

Before each experiment, a cycle of calcium assembly-disassembly was done to remove any inactive protein. EcFtsZ protein was in lysis buffer plus 300 mM KAc, or in HMK buffer (50 mM HEPES, pH 7.7, 5 mM MgAc, 100 mM KAc). 10 mM $CaCl_2$ and 2 mM GTP were added, and the mixture was incubated for 5 min at 37 °C to assemble protofilament bundles. The EcFtsZ polymer was collected by centrifugation at 45,000 rpm for 30 min (Beckman TLA100 rotor). The pellet was resuspended in the appropriate buffer and centrifuged again to remove any insoluble protein. Most experiments were done in HMK buffer, which is close to the physiological condition of bacterial cytoplasm. To test the assembly without Mg, we used MEK buffer (50 mM MES, pH 6.5, 1 mM EDTA, 100 mM KAc; the pH was lowered to 6.5 because EcFtsZ assembles very poorly at pH 7.7 without Mg).

Most assays used the tryptophan-induced ATTO fluorescence quenching developed previously (18). ATTO fluorescence can be efficiently quenched by a tryptophan that is close enough to form van der Waals contacts or ring stacking (19, 20). We constructed the EcFtsZ double mutant T151C/Y222W, in which the cys is ~10 Å from the trp. We labeled the cys with the fluorescent dye ATTO-655-maleimide (Fluka). For assembly experiments, the labeled EcFtsZ protein was diluted with a 9-fold excess of wild type FtsZ to avoid the formation of bundles. Assembly kinetics were measured at the ATTO peak emission 680 nm, with excitation at 650 nm. The ATTO fluorescence increased as EcFtsZ assembled, presumably due to a small conformational change in the subunits upon assembly (18). All fluorescence measurements were done in a thermostatically controlled cell at 25 °C.

Another assay used FRET, in which PaFtsZV324C was labeled with fluorescein (donor) and tetramethylrhodamine (acceptor). Assembly was tracked by the decrease in donor fluorescence at 515 nm, with excitation at 470 nm as described previously (17, *Chen, 2009 #8469*, 21).

GTPase activity measurement

GTPase activity was measured using a continuous, regenerative coupled GTPase assay (22) (22,(23). In this assay, all free GDP in solution is rapidly regenerated into GTP, and the GTP

hydrolysis rate is measured by the decrease in absorption of NADH. Measurements were made in a thermostatically controlled cell at 25° C.

Electron Microscopy

FtsZ filaments were imaged by negative stain electron microscopy (EM). Approximately 10 µL of sample in the appropriate buffer was incubated with GTP for 1–2 min, or with GMPCPP for 3–4 min and applied to a carbon-coated copper grid. Samples were stained with 2% uranyl acetate and imaged at 50,000X magnification in a Philips 420 electron microscope.

Isothermal Titration Calorimetry (ITC)

The FtsZ-SulA binding affinity was measured at 25 °C using a Microcal VP-ITC microcalorimeter (MicroCal Inc., MA). The samples were prepared in the HMK or MEK buffer and degassed using a Microcal ThermoVac. The sample cell contained 1.45 ml of 3 µM SulA, and each titration was 10 µl of 30 µM FtsZ. The titration data were fitted using the "one set of sites model" MicroCal software package to calculate the binding affinity.

The 30 µM FtsZ-GDP in the syringe would be expected to assemble into short, isodesmic oligomers (24). When these are diluted into the sample chamber they will disassemble, and this will have its own heat of reaction. However, since the FtsZ is immediately sequestered by the excess SulA, the concentration of free FtsZ in the sample chamber will remain low and the heat from the disassembly of GDP-FtsZ oligomers will be identical for each injection. This can then be ignored in the titration of SulA.

Assembly and SulA inhibition in DEAE dextran

In HMK buffer, 5 µM wild type FtsZ or the mutant D212G was mixed with 0, 5 or 10 µM SulA, and 0.1 mg/ml DEAE dextran, and assembly initiated by adding 1 mM GTP. After two min the samples were centrifuged at 20,000 g for 15 min, and the supernatants and pellets were run on 10% SDS-PAGE.

RESULTS

Inhibition of FtsZ by SulA from E. coli

Figure 1 shows assembly of EcFtsZ assayed by EM with or without MBP-SulA protein. EcFtsZ assembled mostly one-stranded filaments in the presence of GTP (Figure 1a). When mixed with equimolar MBP-SulA filament, assembly was abolished (Figure 1b). Assembly in GMPCPP, a slowly hydrolysable GTP analog, produced longer one-stranded filaments and some filament bundles (Figure 1c). Assembly in GMPCPP was substantially inhibited, but not completely blocked, by an equimolar or two-fold excess of MBPSulA (Figure 1d,e). Assembly in MEK buffer, where Mg is replaced with EDTA, gave long, onestranded filaments (Fig. 1f). In this buffer MBP-SulA only partially inhibited assembly (Fig. 1g). These results contradict the report of Dajkovic et al (14) that MBP-SulA did not inhibit assembly in GMPCPP or EDTA.

The assembly of FtsZ is accompanied by hydrolysis of GTP, and GTPase activity provides an alternative assay of assembly. To explore the inhibition more quantitatively, we assayed the GTPase for increasing concentrations of EcFtsZ, and in the presence of different amounts of MBP-SulA. In the absence of MBP-SulA, the GTPase showed a linear increase of 6.7 GTP hydrolyzed per minute per FtsZ above a critical concentration (Cc) of 0.72 µM (Fig. 2b, table 1). The primary effect of MBP-SulA was to increase the apparent Cc (CcApp), to 1.54 µM at 1 µM SulA, and to 3.15 µM at 5 µM SulA, with minimal change in the slope of the line above the CcApp. Note that the increase in CcApp is somewhat less

than the amount of MBP-SulA. This is also different from the report of Dajkovic et al, where the increase in CcApp was approximately equal to the amount of SulA (14).

We confirmed these results using our recently developed assay based on quenching ATTO-655 fluorescence by a nearby trp (18). Note that in the previous study we found that the ATTO label promoted protofilament bundling. To avoid this complication there, as well as in the present study, we used the ATTO-labeled protein as a dilute label, with a 9-fold excess of wild type protein. Thus the assembly is dominated by the wild type protein, and kinetics were identical to those of other trp mutants (18). Fig. 3a and 3b show the EcFtsZ assembly kinetics at different concentration of EcFtsZ without or with 1 μM SulA. In Fig. 3a the curve for 6 μM EcFtsZ shows an overshoot peak at ~10 s, declining to a plateau at ~20 s. We do not understand the structural basis for the overshoot. Fig. 3b shows that SulA inhibited the assembly as assayed by ATTO fluorescence. Figure 3c plots the steady state assembly as a function of increasing concentration of EcFtsZ, and different concentrations of SulA. The results are in excellent agreement with the GTPase assay. The CcApp values for all assays are listed in Table 1.

The ATTO quenching assay provided a means to measure the inhibition of assembly by SulA in GMPCPP and in EDTA. In both cases the effect of SulA was primarily to shift the CcApp. In GMPCPP the CcApp were also shifted by SulA but the shifts were less than for assembly in GTP (Fig. 3d). In MEK buffer (without Mg), the Cc without SulA was much higher, 2.47 μM, and the shifts in SulA were even smaller (Fig. 3e). These results confirmed the EM observation, which showed a major inhibition of assembly in GTP, somewhat less inhibition of assembly in GMPCPP, and only a modest inhibition of assembly in EDTA. The reduced inhibition in MEK buffer was due to the absence of Mg, not the pH, since we found inhibition was similar at pH 7.7 and 6.5 in 5 mM Mg.

The experiments in Fig. 3 measured the inhibition of assembly when FtsZ was pre-mixed with SulA. We next assayed the ability of SulA to disassemble preassembled protofilaments. Fig. 4 compares the disassembly induced by SulA, to that induced by excess GDP. Disassembly of the Mg-GTP polymers occurred in ~ 10 s (this is the time to 1/e of the final plateau, from an exponential fit), while disassembly of GMPCPP and EDTA polymers took ~20s, consistent with their reduced subunit exchange. In all cases the extent of disassembly was somewhat less for SulA than for GDP, and this difference was larger for EDTA, consistent with reduced inhibition seen by EM. Importantly, the kinetics of disassembly induced by GDP and SulA were identical in each case. We have previously interpreted GDP-induced disassembly to be a sequestration mechanism (17, 21), so this suggests a similar mechanism for SulA.

Direct measure of K_A for FtsZ-SulA binding by ITC

All of these results suggest that the mechanism of inhibition involves SulA binding to FtsZ monomers and blocking them from assembly. To understand the mechanism quantitatively we need to know the association constant for SulA binding FtsZ. Below we will deduce this indirectly, but for a direct measure we turned to ITC. Fig. 5 shows the data and the fitting, which gave a K_A of 1.29 μM^{-1}. We attempted to measure the K_A in MEK buffer but the association was much weaker, and we obtained no meaningful data at the maximum protein concentrations available.

FtsZ and SulA from P. aeruginosa

The binding of FtsZ and SulA is well characterized by a crystal structure of the proteins from *P. aeruginosa* (13), but the inhibition of FtsZ assembly by SulA has not been studied for the *Pseudomonas* proteins. We first checked the assembly properties of PaFtsZ.

Interestingly, we found PaSulA assembled a novel helical structure without GTP (Fig. 6c). Centrifugation analysis showed that these were only a small fraction of the total FtsZ. The helices had a diameter of about 15 nm and a pitch of about 19 nm. These helices are similar to but smaller than the helices assembled by EcFtsZ in DEAE-dextran, which had a diameter of 23 nm and a pitch of 21 or 28 nm (25). Also, these helical polymers assembled without stabilization by DEAE dextran.

When GTP was added, the PaFtsZ assembled thin protofilaments very similar to those of EcFtsZ (Fig. 6a). EM showed that PaSulA strongly inhibited the assembly of PaFtsZ, virtually eliminating the protofilaments (Fig. 6b). Unlike EcFtsZ, PaFtsZ assembled poorly in the MEK buffer. EM also showed that PaFtsZ could assemble into long filaments in GMPCPP, and this assembly was also inhibited by a two-fold excess of SulA, but not as strongly inhibited as in GTP.

We next assayed the GTPase activity of PaFtsZ in various concentrations of PaSulA. In the absence of SulA PaFtsZ hydrolyzed ~7.8 GTP per min (Fig. 7a), slightly higher than the 6.7 GTP per min of EcFtsZ (each of these values is from the slope of the curve above the Cc). Increasing concentrations of SulA progressively inhibited the GTPase, primarily by increasing the CcApp, the same as for EcFtsZ. The shifts were larger than in the *E. coli* system, indicating a stronger binding of PaSulA to PaFtsZ.

We then used a FRET assay to determine the kinetics of filament disassembly by PaSulA. PaFtsZ has two cysteines, but we found that labeling either of them with a fluorophore blocked assembly. We therefore changed both cysteines to serines, and mutated V324 to cysteine. EM showed that this mutant PaFtsZV324C could assemble well both unlabeled and after labeling with fluorophores (data not shown). We labeled PaFtsZV324C with fluorescein maleimide as donor and tetramethylrhodamine maleimide as acceptor to set up the FRET assay, similar to the one we have used previously with EcFtsZ (17). Fig. 7b shows a rapid drop in donor fluorescence following addition of GTP, corresponding to protofilament assembly followed by a slower decrease that may be due to filament bundling. Filament bundling was confirmed by EM and a significantly reduced steady-state GTPase activity. We therefore did not use this FRET assay for assembly and CcApp, but it was useful for disassembly studies. Addition of excess SulA or GDP caused a rapid rise in donor fluorescence, indicating rapid disassembly. The kinetics of disassembly were the same when induced by SulA or GDP, suggesting a similar sequestration mechanism for each.

SulA inhibits filament assembly of GTPase-deficient FtsZ mutant D212G

In the presence of GTP, the EcFtsZ mutant D212G forms one-stranded protofilaments in HMK buffer (Figure 8a). When D212G was mixed with equimolar SulA, filament assembly was reduced (Figure 8b), and a two-fold excess of SulA completely abolished assembly (Figure 8c). These results agree with previously published reports that SulA is able to bind D212G (11, 12).

To examine D212G filament disassembly, we used the ATTO 655 quenching assay. For these assays, 10% ATTO 655 labeled FtsZ (T151C Y222W) was mixed with 90% unlabeled D212G. The ATTO-labeled FtsZ is below the Cc for assembly, so it only reports co-assembly with D212G; the assembly will therefore be dominated by D212G. Filament assembly was initiated by the addition of GTP (Figure 8d). Once a steady state was reached, either GDP or SulA was added and the disassembly was monitored by a decrease in ATTO 655 fluorescence. Similar to wild-type FtsZ, the disassembly of D212G was slightly less in amplitude for SulA than for GDP. Importantly, the disassembly rates were the same. These results suggest that SulA and GDP initiate disassembly of the GTPase-dead D212G by a similar mechanism.

We also used the ATTO 655 quenching assay to measure the Cc of D212G and the CcApp of D212G and SulA (Figure 8e). The Cc of D212G was 2.2 µM, significantly higher than that of wild type FtsZ. The CcApp increased to 4 µM in the presence of 3 µM SulA.

Finally, we tested the ability of SulA to inhibit assembly stabilized by DEAE dextran. Fig. 8f shows that SulA substantially inhibited the polymerization of wild type FtsZ, but only slightly inhibited the polymerization of D212G at 10 µM. This agrees with the previous study of Trusca et al (12). The observation that SulA inhibits assembly of D212G protofilaments, but not of tubes stabilized by DEAE dextran is probably explained by our model of balanced equilibrium between (a) FtsZ assembly into polymer and (b) its binding SulA, as developed in the next section. The resistance of the DEAE-dextran polymers suggests that assembly with DEAE dextran is of higher affinity than without, tilting the balance toward assembly rather than sequestration by SulA.

Model of SulA inhibition used to estimate the binding affinity of FtsZ-SulA

We will show here that a simple sequestration mechanism is consistent with our data, and that we can use the shift in apparent Cc to calculate the K_D for FtsZ-SulA association. We will use the term Cc for the critical concentration in the absence of SulA. This is the reciprocal of the association constant for adding a subunit to a protofilament, and equals the concentration of free FtsZ in apparent equilibrium with filament ends at steady state. Cc is assumed not to change in the presence of SulA. SulA is assumed to cause an increase in the apparent critical concentration, CcApp, by sequestering the FtsZ to which it is bound: CcApp = Cc +[ZS], where [ZS] is the concentration of the FtsZ-SulA complex at steady state. If SulA bound FtsZ with high affinity, we would expect the CcApp to be increased by exactly the amount of SulA added, since the equivalent amount of FtsZ would be sequestered. This was the result reported by Dajkovic et al (14). In our experiments the CcApp was increased by the addition of SulA, but the increase was always less than the total amount of SulA. This suggests that the binding of SulA to FtsZ is of modest affinity, and sets up a competition between binding of FtsZ to the protofilament ends and binding to SulA.

$$Z + Zp <-> Zp+1 \quad [Z]=Cc \quad (1)$$

[Z] is the concentration of free FtsZ subunits at steady state, not bound to SulA, and is equal to Cc.

$$Z + S <-> ZS \quad [ZS]=K_{AS}[Z][S], \quad (2)$$

where [ZS] is the concentration of FtsZ-SulA complex, and K_{AS} is the association constant for forming the complex.

The concentration of free SulA in solution, [S], is equal to the total concentration [S_t] minus the amount bound to FtsZ

$$[S]=[S_t]-[ZS] \quad (3)$$

Inserting (1) and (3) into equation (2)

$$[ZS]=K_{AS}Cc([S_t]-[ZS]); \; [ZS]=\frac{K_{AS}CcS_t}{1+K_{AS}Cc} \quad (4)$$

We can now write

$$CcApp=Cc+[ZS]=Cc+\frac{K_{AS}CcS_t}{1+K_{AS}Cc} \quad (5)$$

$$K_{AS}=\frac{CcApp-Cc}{CcS_t-CcAppCc+Cc^2} \quad (6)$$

We can now use equation 6 to calculate K_{AS} for each value of CcApp determined from the GTPase assays or assembly assayed by ATTO fluorescence. The calculated values are given in Table 1, where we have used $K_{DS} = 1/K_{AS}$ in units μM. These K_{DS} values can be compared directly with Cc, the dissociation constant for assembly of a subunit onto a protofilament (Cc = CcApp for 0 SulA). The K_{DS} for 1 μM SulA (in parentheses) is considered less accurate because of the small shift. Values for 3 and 5 μM SulA binding to wild type FtsZ, 0.53 and 0.62, are very close to the K_{DS} from the ITC measurement, 0.78 μM. The values from polymer assay by ATTO fluorescence are similar those from the GTPase assay. We should also note that during our ITC measurement, no GTP was added and FtsZ should be monomeric with a small excess of GDP. This suggests that SulA binds to FtsZ with similar affinity in the GDP and GTP bound states. The reduced inhibition by SulA for assembly in GMPCPP or EDTA can be explained by a reduced affinity for binding SulA in these conditions. The binding affinity of SulA for EcFtsZ appears to be reduced 3–4 fold for assembly in GMPCPP and for assembly of D212G, and is reduced more than 10-fold in EDTA (Table 1). This is consistent with our inability to measure a K_{AS} by ITC in EDTA, and explains why SulA only weakly inhibits FtsZ assembly in EDTA. Finally the affinity of SulA for PaFtsZ is 3–5 fold higher than for EcFtsZ.

DISCUSSION

Our work is consistent with the model that SulA inhibits FtsZ by binding to the assembly site of FtsZ subunits and sequestering them from the assembly reaction. We add one important parameter not previously considered – the association constant K_{AS} for the reversible binding of SulA to FtsZ. For EcFtsZ assembly in HMK with GTP, this is the same order of magnitude as the binding of FtsZ subunits to protofilament ends, so the assembly needs to be treated as a competition of these two reactions. Importantly, the K_{AS} measured by ITC is very close to that deduced from the model for EcFtsZ assembly in GTP.

We show here by EM that D212G assembles one-stranded protofilaments similar to wild type. These results contradict earlier work by Mukherjee et al (11), who reported that D212G did not polymerize except with an excess of wild type FtsZ. However, they examined filament formation under different conditions (50 mM Mes-NaOH pH 6.5, 10 mM $MgCl_2$ and 200 mM KCl). Under these conditions, primarily due to the pH 6.5, vs our more physiological pH 7.7, we also could not detect filament formation of D212G. The ATTO fluorescence assay confirmed and quantitated the assembly. Assembly of D212G was inhibited by SulA. When assembly was stabilized by DEAE dextran, assembly of wild type FtsZ was largely inhibited by a two-fold excess of SulA, while D212G was only slightly inhibited, in agreement with the previous study of Trusca et al (12).

Our data contradict the previous conclusion that assembly in GMPCPP or in EDTA was not inhibited at all by SulA. Our EM shows qualitative inhibition of assembly under both conditions, and our ATTO fluorescence assay confirms the inhibition with extensive quantitative data. The inhibition of assembly in GMPCPP was less than the inhibition in GTP, in qualitative agreement with Dajkovic et al (14). Our model estimates a 3–4-fold reduced affinity of SulA for FtsZ-GMPCPP, relative to FtsZ-GTP. This is a small change (0.5 kcal/mol), and may reflect problems in the indirect calculation from CcApp, rather than an actual change in K_D. A similar ~3-fold reduction in assembly was calculated from the inhibition of D212G, which also has minimal GTPase activity and reduced subunit turnover. It is clear from Table 1 that the calculation gives inconsistent results at low FtsZ concentrations, and it may also show deviation for reduced subunit turnover.

The mutant D212G was originally isolated as dominant inhibitor of SulA, and designated "resistant to SulA" (26). This would seem to contradict our finding that assembly of D212G is sensitive to SulA. However, in the original isolation step and subsequent testing, the mutant D212G was expressed from a phage or plasmid in the presence of wild type FtsZ from the genome (26). There are two ways a plasmid-expressed mutant FtsZ can generate resistance to SulA. One is that the mutation blocks the binding site for SulA. Then the plasmid-expressed mutant FtsZ is immune to SulA and can function for cell division. This happens for F268C, which is in the middle of the SulA-binding site (13). The other mechanism is that the mutant FtsZ can bind SulA and is expressed in sufficient quantity to sequester most of the SulA, leaving the wild type FtsZ free to continue cell division. This is apparently the case for D212G, which is outside the SulA-binding site (13).

We found that the inhibition of assembly by SulA was even weaker in EDTA, but still measurable. The weaker inhibition could be attributed to a >10-fold reduction in affinity of SulA for EcFtsZ in the absence of Mg. This suggests that binding of SulA to FtsZ might require binding of Mg; however no Mg was seen in the crystal structure of PaFtsZ-SulA (13). The FtsZ subunit may have a different conformation in EDTA, since the dimer nucleus was much weaker relative to elongation in EDTA than in Mg (16, 17).

Our model is simpler than the one suggested by Dajkovic et al (14). It has only two parameters: the Cc for association of FtsZ subunits onto the end of protofilaments, and the association constant K_{AS} for forming the SulA-FtsZ complex. The previous model had an implicit assumption that this association was much stronger than that of protofilament assembly, which fit the centrifugation data showing that CcApp was equal to Cc plus the total added SulA. Our quantitative GTPase assays and fluorescence assays show that CcApp is always less than this, and the difference can be used to measure K_{AS}. In the one case we were able to measure K_{AS} by ITC it was very close to the value deduced from the model (0.78 μM from ITC vs 0.68–0.78 μM for the model).

Acknowledgments

ABBREVIATIONS

GMPCPP	Guanosine-5′-[(αβ)-methylene]triphosphate
Cc	critical concentration
CcApp	apparent critical concentration

FRET	Förster resonance energy transfer
ITC	isothermal titration calorimetry
EM	electron microscopy
EDTA	Ethylenediaminetetraacetic acid

References

1. Osawa M, Anderson DE, Erickson HP. Reconstitution of contractile FtsZ rings in liposomes. Science (New York, NY). 2008; 320:792–794.

2. Osawa M, Anderson DE, Erickson HP. Curved FtsZ protofilaments generate bending forces on liposome membranes. The EMBO journal. 2009; 28:3476–3484. [PubMed: 19779463]

3. Osawa M, Erickson HP. Inside-out Z rings - constriction with and without GTP hydrolysis. Molec Microbiol. 2011; 81:571–579. [PubMed: 21631604]

4. Erickson HP, Anderson DE, Osawa M. FtsZ in Bacterial Cytokinesis: Cytoskeleton and Force Generator All in One. Microbiol Mol Biol Rev. 2010; 74:504–528. [PubMed: 21119015]

5. Adams DW, Errington J. Bacterial cell division: assembly, maintenance and disassembly of the Z ring. Nature reviews. 2009; 7:642–653.

6. Huisman O, D'Ari R, Gottesman S. Cell-division control in Escherichia coli: specific induction of the SOS function SfiA protein is sufficient to block septation. Proceedings of the National Academy of Sciences of the United States of America. 1984; 81:4490–4494. [PubMed: 6087326]

7. Huisman O, D'Ari R. An inducible DNA replication-cell division coupling mechanism in E. coli. Nature. 1981; 290:797–799. [PubMed: 7012641]

8. Bi E, Lutkenhaus J. Cell division inhibitors SulA and MinCD prevent formation of the FtsZ ring. J Bacteriology. 1993; 175:1118–1125.

9. Lutkenhaus JF. Coupling of DNA replication and cell division: sulB is an allele of ftsZ. Journal of Bacteriology. 1983; 154:1339–1346. [PubMed: 6343351]

10. Higashitani A, Higashitani N, Horiuchi K. A cell division inhibitor SulA of Escherichia coli directly interacts with FtsZ through GTP hydrolysis. Biochemical and Biophysical Research Communications. 1995; 209:198–204. [PubMed: 7726836]

11. Mukherjee A, Cao C, Lutkenhaus J. Inhibition of FtsZ polymerization by SulA, an inhibitor of septation in Escherichia coli. Proc Natl Acad Sci U S A. 1998; 95:2885–2890. [PubMed: 9501185]

12. Trusca D, Scott S, Thompson C, Bramhill D. Bacterial SOS checkpoint protein SulA inhibits polymerization of purified FtsZ cell division protein. J Bacteriol. 1998; 180:3946–3953. [PubMed: 9683493]

13. Cordell SC, Robinson EJ, Lowe J. Crystal structure of the SOS cell division inhibitor SulA and in complex with FtsZ. Proc Natl Acad Sci U S A. 2003; 100:7889–7894. [PubMed: 12808143]

14. Dajkovic A, Mukherjee A, Lutkenhaus J. Investigation of regulation of FtsZ assembly by SulA and development of a model for FtsZ polymerization. J Bacteriol. 2008; 190:2513–2526. [PubMed: 18245292]

15. Sontag CA, Sage H, Erickson HP. BtubA–BtubB heterodimer is an essential intermediate in protofilament assembly. PLoS ONE. 2009; 4:e7253. [PubMed: 19787042]

16. Chen Y, Bjornson K, Redick SD, Erickson HP. A rapid fluorescence assay for FtsZ assembly indicates cooperative assembly with a dimer nucleus. Biophysical journal. 2005; 88:505–514. [PubMed: 15475583]

17. Chen Y, Erickson HP. Rapid in vitro assembly dynamics and subunit turnover of FtsZ demonstrated by fluorescence resonance energy transfer. J Biol Chem. 2005; 280:22549–22554. [PubMed: 15826938]

18. Chen Y, Erickson HP. Conformational changes of FtsZ reported by tryptophan mutants. Biochemistry. 2011; 50:4675–4684. [PubMed: 21510681]

19. Doose S, Neuweiler H, Sauer M. Fluorescence quenching by photoinduced electron transfer: a reporter for conformational dynamics of macromolecules. Chemphyschem. 2009; 10:1389–1398. [PubMed: 19475638]

20. Mansoor SE, Dewitt MA, Farrens DL. Distance mapping in proteins using fluorescence spectroscopy: the tryptophan-induced quenching (TrIQ) method. Biochemistry. 2010; 49:9722–9731. [PubMed: 20886836]

21. Chen Y, Erickson HP. FtsZ filament dynamics at steady state: subunit exchange with and without nucleotide hydrolysis. Biochemistry. 2009; 48:6664–6673. [PubMed: 19527070]

22. Ingerman E, Nunnari J. A continuous, regenerative coupled GTPase assay for dynamin-related proteins. Methods Enzymol. 2005; 404:611–619. [PubMed: 16413304]

23. Chen Y, Erickson HP. In Vitro Assembly Studies of FtsZ/Tubulin-like Proteins (TubZ) from Bacillus Plasmids: EVIDENCE FOR A CAPPING MECHANISM. J Biol Chem. 2008; 283:8102–8109. [PubMed: 18198178]

24. Rivas G, Lopez A, Mingorance J, Ferrandiz MJ, Zorrilla S, Minton AP, Vicente M, Andreu JM. Magnesium-induced linear self-association of the FtsZ bacterial cell division protein monomer. The primary steps for FtsZ assembly. J Biol Chem. 2000; 275:11740–11749. [PubMed: 10766796]

25. Lu C, Reedy M, Erickson HP. Straight and curved conformations of FtsZ are regulated by GTP hydrolysis. J Bacteriol. 2000; 182:164–170. [PubMed: 10613876]

26. Bi E, Lutkenhaus J. Analysis of ftsZ mutations that confer resistance to the cell division inhibitor SulA (SfiA). J Bacteriology. 1990; 172:5602–5609.

27. Lu C, Stricker J, Erickson HP. Site-specific mutations of FtsZ - effects on GTPase and in vitro assembly. BMC Microbiol. 2001; 1:7. [PubMed: 11394965]
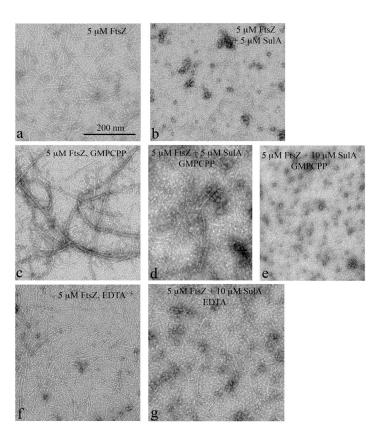
Figure 1.
EM images of EcFtsZ without SulA and with the indicated addition of SulA. (a, b) in HMK buffer with GTP; (c, d, e) in HMK with GMPCPP; and (f, g) in MEK buffer with GTP.
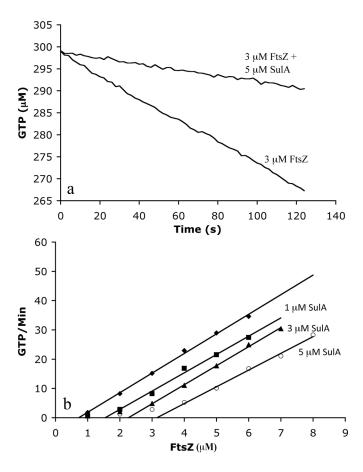
Figure 2.
Inhibition of GTPase of EcFtsZ by SulA. (a) 3 μM EcFtsZ hydrolyzed GTP at a rate of about 15 GTP/min, which was reduced to about 3 GTP/min after adding 5 μM SulA. (b) The GTPase measured at increasing concentration of EcFtsZ shows that SulA increases the apparent critical concentration.
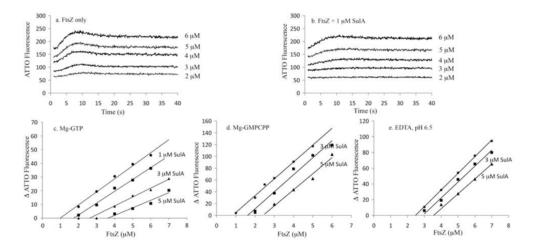
Figure 3.
Assembly assayed by increase in ATTO fluorescence. EcFtsZ assembly kinetics at different concentration of EcFtsZ without (a) and with 1 µM SulA (b). (c) To measure CcApp, ATTO fluorescence before adding GTP was subtracted from the fluorescence at steady state. For the curve without SulA steady state fluorescence was averaged from 25–28 s, to avoid the overshoot (a). For curves with SulA the overshoot was minimal (b), and steady state was measured from 10–13 s. The assay was repeated for assembly in HMK plus GMPCPP (d) and in MEK buffer plus GTP (e).
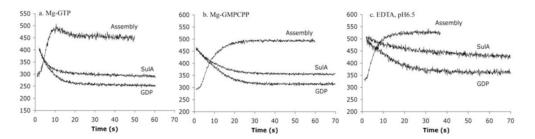
Figure 4.
The assembly and disassembly of ATTO-FtsZ filaments induced by excess GDP or excess SulA. (a) Assembly in HMK buffer plus GTP; (b) in HMK plus GMPCPP; and (c) MEK plus GTP. The EcFtsZ concentration was 5 µM, SulA concentration was 10 µM and GDP was 2 mM. The assembly curve shows the initial assembly induced by addition of 0.1 µM GTP or GMPCPP. At the end of that assembly SulA or GDP was added, and the disassembly was plotted as a decrease in fluorescence (these curves are shifted back to the zero time point, although there was a 1–2 s delay between the addition of SulA and the start of the fluorescence measurement.)
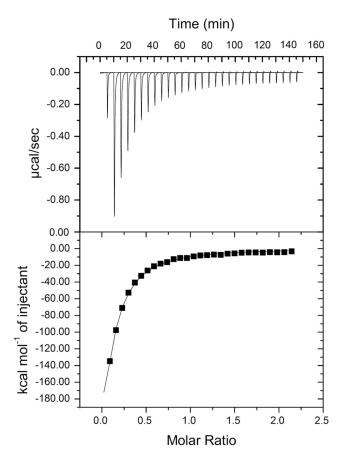
Figure 5.
The binding of EcFtsZ and SulA measured by ITC. See Methods for details of the assay.
The curve fit gives the K_A as 1.29 μM^{-1} (K_D = 0.78 μM). For this measurement the proteins were in HMK buffer with no GTP.
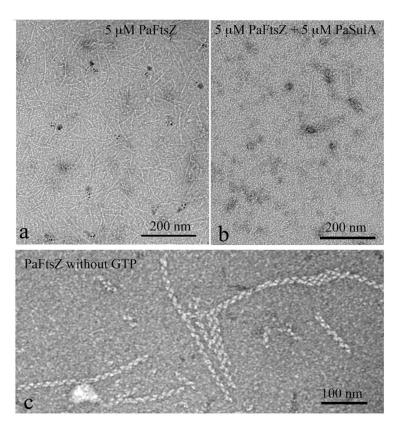
Figure 6.
EM images of PaFtsZ and the inhibition of assembly by SulA. (a) 5 μM PaFtsZ assembled into one-stranded protofilaments in GTP. (b) After adding 5 μM SulA, most filaments disappeared. (c) A new polymer structure was found for PaFtsZ without added nucleotide (or in the presence of GDP). The ~15 nm diameter is smaller than the 23 nm diameter of EcFtsZ minirings and DEAE dextran tubes.
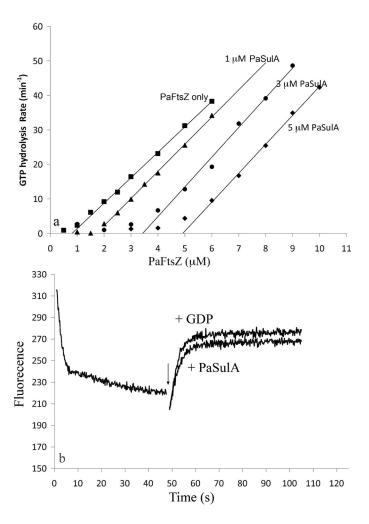
Figure 7.
(a) GTPase of PaFtsZ is inhibited by SulA, primarily as an increase in the apparent critical concentration. (b) Assembly of 5 µM PaFtsZ assayed by FRET. Assembly results in a drop in donor fluorescence. Upon addition of SulA or GDP there was a small drop in fluorescence due to the ~10% dilution, and then the donor fluorescence increased, indicating disassembly. The rate of disassembly is the same for GDP and SulA.
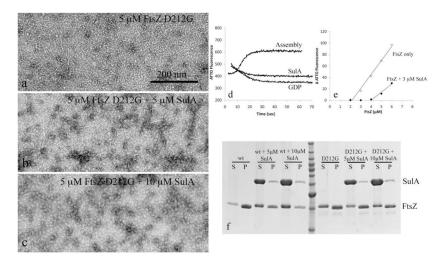
Figure 8.
SulA inhibits assembly of EcFtsZ D212G. EM images of 5 µM Ec FtsZ D212G in HMK buffer with 1 mM GTP (a) and mixed with 5 µM (b) or 10 µM (c) SulA. Scale bar: 200 nm. Assembly and disassembly of 4.5 µM Ec D212G plus 0.5 µM ATTO-FtsZ (d). Assembly was initiated by the addition of 100 µM GTP. Disassembly was induced with either 2 mM GDP or 10 µM SulA. (e) The critical concentration of Ec FtsZ D212G was assayed by measuring the increase in ATTO fluorescence, using a 9:1 mix of D212G:ATTO-FtsZ. (f) SulA inhibition of assembly in DEAE dextran.

Table 1

The FtsZ apparent critical concentration as a function of SulA, in different assembly conditions. The dissociation constant $K_{DS} = 1/K_{AS}$, was calculated from eq. 6.

Buffer (assay)	SulA (μM)	Capp (μM)	K_{DS} (μM)
HMK-GTP (ITC)			0.78
HMK-GTP (GTPase)	0	0.72	
	1	1.54	(0.16)
	3	2.26	0.68
	5	3.15	0.76
HMK-GTP (ATTO)	0	0.81	
	1	1.73	(0.07)
	3	2.62	0.53
	5	3.64	0.62
GMPCPP (ATTO)	0	0.83	
	3	1.61	2.47
	5	2.41	1.91
MEK (ATTO}	0	2.47	
	3	2.90	16.51
	5	3.55	10.72
PaFtsZ (GTPase)	0	0.81	
	1	1.72	(0.08)
	3	3.44	0.11
	5	4.92	0.18
D212G (ATTO)	0	2.2	
	3	4.0	1.47